JETIR.ORG ISSN: 2349-5162 | ESTD Year : 2014 | Monthly Issue
JOURNAL OF EMERGING TECHNOLOGIES AND INNOVATIVE RESEARCH (JETIR)
An International Scholarly Open Access, Peer-reviewed, Refereed Journal

CANCER DETECTION BY ARTIFICIAL INTELLIGENCE

By leveraging machine learning algorithms and deep learning models, AI system can detect subtle anomalies in medical images, such as X-rays, MRIs and CT scans. This technology supports personalized treatment planning and reducing the burden on healthcare system.

[1]Rakshitha Rai, [2]Dr. Sandeep Bhat
[1]M.Tech Student, [2]Professor, Department of
Computer Science and Engineering,
Computer Science and Engineering
Srinivas Institute of Technology, Valachil, Mangaluru, Karnataka, India

Abstract: Artificial intelligence (AI) has become increasingly promising in cancer research, particularly for detection and staging. This review examines AI's role in interpreting imaging data from modalities like MRI, CT, and ultrasound, highlighting its accuracy in identifying tumor regions, size, and grade. It covers AI applications across 12 cancer types, includes breast, prostate, and lung cancers, and summarizes current challenges. CT and ultrasound emerged as ideal for detection, while MRI aids staging. The review offers a roadmap for leveraging AI to improve early cancer diagnosis and patient outcomes.

I. INTRODUCTION

Normal cells respond to the body's signals to grow, divide, or die, but lifestyle-induced genetic changes can disrupt these processes, leads to uncontrolled cell growth and cancer. These abnormal cells form tumors that may spread to multiple parts of the body. Cancer is responsible for one in six deaths globally. Diagnosis methods include blood tests, biopsies, and medical imaging, with AI playing a growing role in the latter. AI uses algorithms to analyze large, complex datasets, improving diagnostic speed and accuracy, reducing errors, and easing radiologists' workloads. It also supports disease monitoring and treatment planning. Despite its benefits, AI adoption in healthcare remains slow due to several challenges.

This reviews focused on the use of AI in medical imaging for cancer diagnosis and performance. AI aids radiologists by interpreting images, identifying cancer locations, and classifying its stages. It also supports clinical workflows, including detection, monitoring, and treatment planning. AI models, established using machine learning and deep learning, analyze complex cancer structures through feature extraction. While AI enhances diagnostic accuracy, it faces challenges such as legal and ethical concerns, lack of standardized datasets, and the need for expert validation. Overtraining models can also lead to inaccurate outcomes.

II. IMPLEMENTATION OF AI IN CANCER

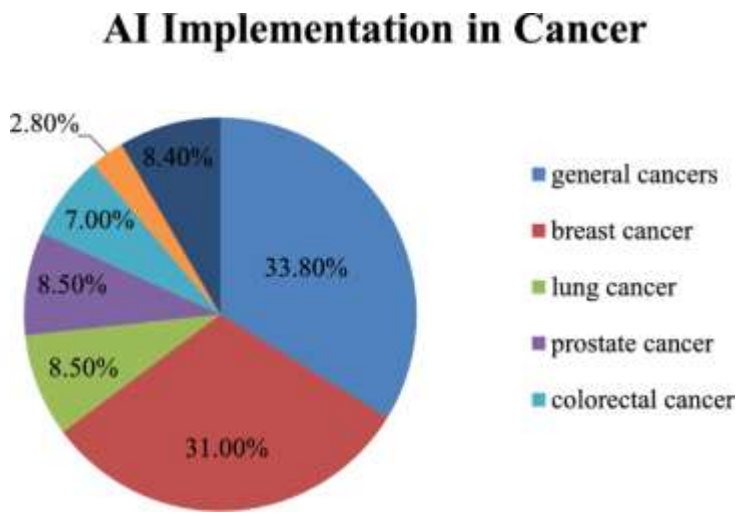

Fig. 1.1 AI Implementations in cancer

1.1 Various Types of Cancer

Cancers can originate from various tissues and differ by type and prevalence. Figures 2a and 2b show that cancers like prostate and lung are more common in men. Diagnosis methods include biopsy, transrectal ultrasound, CT, and MRI, with MRI often used to assess cancer progression. Prostate cancer can also be diagnosed through histopathological analysis, graded using the Gleason system. However, due to the cancer's slow growth, Gleason-based risk analysis can be limited. In 2014, the International Society of Urological Pathology revised this grading into five distinct groups for improved classification.

1.1.1 Bladder Cancer

According to WHO 2020 data, bladder cancer accounts for 3.2% of all cancers. It typically begins in the bladder's inner lining and is treatable in early stage, however can progress to deeper layers and spread if not managed. Recurrence is common, making regular monitoring essential (1). Bladder cancer types include urothelial carcinoma, squamous cell carcinoma, and adenocarcinoma, and are classified based on invasion depth as non-muscle invasive, muscle invasive, or metastatic. MRI is the preferred imaging method, though challenges arise due to bladder size, shape, and urine-related image distortion.

1.1.2 Prostate Cancer

Prostate cancer one of the most common life-threatening cancer in men, with 1.41 million new cases in 2020, accounting for 7.8% of all cancers. It is the one of the leading cause of cancer death in men, though early detection leads to over 90% recovery. Lung cancer had 2.2 million new cases in 2020, primarily distressing smokers. It is classified into non-small cell lung cancer (NSCLC, ~80% of cases) and small cell lung cancer (SCLC, 10–15%). NSCLC including squamous cell carcinoma, adenocarcinoma, and large cell carcinoma (2). Diagnosis involves chest X-ray, CT, PET-CT, and biopsy.

1.1.3 Lung Cancer

Lung cancer develop from abnormal cell growth in the bronchioles and alveoli and can also effect from cancer spreading from other organs. It is the second most common cancer in the global, accounting for 12.2% of cases. Thyroid cancer arises from the growth of thyroid cells, forming either benign or malignant nodules. Main types include thyroid, medullary, and anaplastic thyroid cancers (2). Diagnosis is typically done using ultrasound, with the Ti-RADS score assessing malignancy risk. MRI and PET method scans are also used for further evaluation.

1.1.4 Kidney Cancer

Kidney cancer, accounting for 2.4% of all cancers, primarily affects adults over 60 and is often curable if detected early. Results are from uncontrolled cell growth in different kidney regions and includes types like renal cell carcinoma (RCC), transitional cell cancer, renal sarcoma, and Wilms tumor (mainly in children). Diagnosis methods include CT, MRI, ultrasound, and renal mass biopsy (1).

1.1.5 Endometrial Cancer

Endometrial (uterine) cancer is the sixth most common cancer in women, making up 6.9% of female cancers, with about 2.8% of women diagnosed. It originates in the endometrium, where fetal development occurs. Early symptoms aid diagnosis, and hysterectomy is the most effective treatment. Imaging methods include CT, MRI, transvaginal, and ultrasound. The cancer is classified into type 1 (grades 1 and 2) and type 2 (grade 3).

1.1.6 Brain Cancer

Brain cancer is abnormal cell growths in the brain, with over 308,000 new cases reported in 2020 (WHO). They can be primary, originating from glioma cells, or secondary, spreading from other body parts. WHO classifies them from grade I to IV. CT and MRI are the main imaging methods used for diagnosis.

1.1.7 Liver Cancer

Liver cancer, responsible for 5% of all cancer cases, is considered fatal due to the liver's vital functions in digestion and detoxification. It often originates from liver or bile duct cells, with common types including hepatocellular carcinoma, intrahepatic cancer (10–20%), and the rare angiosarcoma. It can also be metastatic, spreading from other organs. Liver cancer ranks sixth in prevalence and is diagnosed using MRI, CT, and ultrasound.

1.1.8 Breast Cancer

Breast cancer is the oe of the common cancer in women and globally, with 2.26 million new cases in 2020, accounting for 12.5% of all cancers (WHO). It begins in the ducts or lobules of the breast and is classified as invasive ductal or invasive lobular carcinoma (1). It can metastasize to other body parts. Screening techniques are including mammography, clinical and self-exams, ultrasound, MRI, digital breast tomography, and biopsy.

1.2 Imaging Technique To Detect Cancer And Prediction

Timely cancer detection is critical for successful treatment, and different methods are used for diagnosis, including physical exams, lab tests, imaging, endoscopy, and biopsy. Non-invasive cancer detection is primarily achieved through imaging modalities like X-rays, CT, MRI, PET, ultrasound, mammography, and endoscopy (3). These techniques help identify the cancer's location, size, and spread, with CT and MRI best for anatomical scans, and PET and SPECT for detecting morphological changes. X-rays are majorly used for diagnosing bone and lung cancers, though they are less effective for soft tissue cancers due to their lower absorption capacity.

1.2.1 X-rays

X-rays create shadow images of tissues and organs and are mostly used to diagnose bone and lung cancers. Modified forms like CT, mammography, and fluoroscopy are also used. X-rays are more effective for hard structures, with less clarity for soft tissues. They can help identify lung, breast, lymphoma, and bone cancers.

1.2.2 CT

A CT scan is an advanced form of X-ray that rotates around the body, capturing images from dissimilar angles to create a 3D cross-sectional view. It is mainly useful for imaging the abdomen but may struggle to define organ functions. CT scans can detect lung, abdominal, gastrointestinal, lymphoma, bone, and metastatic cancers.

1.2.3 MRI

MRI is a non-invasive imaging system that doesn't use radiation. It is especially effective for imaging soft tissues like the brain, muscles, and ligaments (3). MRI can detect brain, spine, breast, prostate, pelvic, liver, and abdominal cancers, as well as assess cancer staging and spread.

1.2.4 Ultrasound

Ultrasound uses high-frequency sound waves to create real-time images, with its depth of penetration depending on the frequency. It is effective for identifying tissues or organs containing liquids and assessing organ function. Ultrasound can diagnose breast, thyroid, liver, pancreatic, and gynecological cancers. A radiologist interprets these images to assist doctors in diagnosis and treatment.

1.3 Problem Statement

Early and accurate cancer detection is critical for effective treatment, but traditional methods like blood tests and biopsies can be time-consuming (2). AI enhances imaging techniques, improving diagnostic accuracy over radiologists. By utilizing large datasets, AI helps in pattern recognition, differentiating normal and abnormal tissues, and identifying cancerous tumors. The journal paper is prepared as follows: Sect. 2 covers the review methodology, Sect. 3 discusses cancer diagnosis through image processing, Sect. 4 examines AI applications in cancer diagnosis, and Sect. 5 concludes the review.

II Cancer Diagnosis with Image Processing Techniques

Image processing aids radiologists and pathologists in cancer diagnosis and reduces human error. The process includes:

- Image Acquisition: Collecting images from various imaging modalities.
- Pre-processing: Enhancing image quality by adjusting contrast, resizing, and reducing noise.
- Feature Extraction: Identifying areas of interest like shape, density, and texture of cancerous nodules.
- Segmentation: Separating cancer-affected tissue for analysis.
- Classification: Using ML and DL techniques to classify segmented areas as cancerous or non-cancerous.
- Validation: Verifying results with AI performance metrics.

III AI Applications used in Diagnosis of Different Cancers

Medical imaging plays a vital role in detecting even the smallest cancerous cells within a specific area. However, each imaging modality come with inherent limitations, such as operational frequency, radiation intensity, radiation characteristics, resolution, contrast, and sensitivity, as outlined. Due to these constraints, only certain imaging techniques are fitting for identifying specific types of cancer. Radiologists rely on the chosen imaging method not only to distinguish the presence of cancer but also to assess its severity and guide subsequent treatment decisions (2). A number of research studies have explored the purpose of machine learning (ML) and deep learning (DL) algorithms diagonally different cancer types using these imaging techniques.

3.1 Breast Cancer

Breast cancer analysis commonly uses ultrasound, mammography, and MRI, each presenting unique challenges. Ultrasound images are often low-contrast and blurry, making tumor detection difficult. Researchers have applied different machine learning (ML) and deep learning (DL) techniques improve detection and classification correctness. Yap et al. tested LeNet, U-Net, and FCN-AlexNet, with FCN-AlexNet performing best. Jian et al. used a two-stage classifier (Adaboost and SVM) with random walk segmentation, achieving 87.5% accuracy. Hu employed a dilated FCN with a phase-based model, reaching 71.9% accuracy and 71.2% sensitivity. Byrra improved performance by converting grayscale ultrasound to RGB using CNNs, achieving an AUC of 0.936. Fujioka et al. used GoogleNet to distinguish tumors with 92.5% accuracy. Huang et al. used ROI-CNN and G-CNN to grade tumors with up to 99.8% accuracy (1).

Mammography-based detection also benefits from AI. Mendel et al. compared DBT and digital mammograms using CNNs and SVMs, achieving AUCs of 0.88 and 0.89. Samala et al. applied multistage transfer learning with CNNs, reaching AUC 0.91. CESM images analyzed by Perek et al. achieved 100% sensitivity. Cai et al. found filtered deep features most effective in classifying calcifications (4). Akselrod-Ballin used XGBoost with DNN, reaching AUC 0.91. Samala's multi-task DCNN outperformed single-task models.

MRI offers the highest detection rate. Antropova used pre-trained CNNs and radiomics across MRI, mammography, and ultrasound, achieving AUCs up to 0.90. LSTM models also showed promise in lesion classification. Huynh et al. demonstrated ensemble classifiers combining CNN and analytical features yield better results (AUC 0.86). Samala used a layered CNN evolution method on DBT for mass classification.

3.2 Brain Cancer

Brain tumors are among the most dangerous diseases due to their potential to increase intracranial pressure and cause severe neurological damage or death. MRI and CT are the main imaging modalities used for diagnosis. Different deep learning and machine learning model has been developed to recover brain cancer detection and classification. Iqbal et al. achieved 82.29% accuracy using a CNN-LSTM ensemble. Mehmood et al. used SVM-based feature extraction and reached 99% accuracy. Saba et al. combined GrabCut segmentation with VGG-19, achieving high Dice similarity scores on BraTS datasets. Shankar et al. applied optimal feature fusion and ANFIS classifier for 96.23% accuracy.

Kang et al. fused CNN features from GoogLeNet, ResNet18, and AlexNet, reaching 99.7% accuracy. Khan et al. used histogram equalization, DCT, and VGG models, achieving up to 97.8% accuracy. Ahmadi's fuzzy wavelet neural network reached 100% accuracy. Other approaches, such as fuzzy C-means clustering, genetic algorithms, and particle swarm optimization, also showed high performance. CNN variations like U-Net, V-Net, and multi-depth fusion models by Deng, Huang, Guan, and Zhang reported Dice scores between 0.68 and 0.90 for different tumor regions.

Amin et al. used stacked sparse autoencoders on BraTS datasets, achieving up to 100% accuracy. Ayadi applied hyperparameter optimization on Inception-ResNet V2 and achieved 99.98% accuracy. Ramzan's 3D CNN segmented brain regions with a mean Dice score of 0.903. Gupta used a three-stage ML classifier system with up to 97.76% accuracy for glioma classification. Russo et al. used ML on PET/CT images for tumor grading, achieving ~85% accuracy on Siemens data and ~70% overall.

3.3 Bladder Cancer

Bladder cancer is primarily assessed using CT and MRI, though AI-based segmentation, especially on MRI, remains underexplored. Garapati et al. used ML techniques (LDA, SVM, RF, NN) on CT data with two-fold cross-validation, achieving ROC scores up to 0.97. Cha et al. developed a DCNN for bladder segmentation using Haar features, with a training error of 0.054. Dolz et al. applied MRI-based segmentation to delineate tumor regions, achieving DSC scores of 0.69 (tumor), 0.98 (inner wall), and 0.84 (outer wall). Cha et al. also used CNNs to evaluate treatment response from CT scans, achieving AUCs of 0.73 and 0.63–0.65 in separate studies.

3.4 Prostate Cancer

Prostate cancer discovery and grading using AI is challenging due to image resolution limitations and anatomical variability. MRI and ultrasound are the primary imaging modalities. Jensen et al. used DWI and T2W MRI with a KNN classifier, achieving AUCs between 0.85 and 0.94. Toivonen et al. reported best results using T2W, ADCm, and K features (AUC 0.88). Antonelli et al. predicted Gleason pattern 4 using ML, with AUCs of 0.83 (peripheral zone) and 0.75 (transition zone). Radhakrishnan et al. applied DBSCAN and SVM on ultrasound images, with combined GLCM and GRLM features outperforming individual methods.

Yuta et al. used hierarchical clustering on multiparametric MRI for tumor classification. Viswanath et al. tested 12 classifiers, finding QDA most accurate. Dominik et al. used 3D CNN on MRI to reduce unnecessary biopsies. Yang et al. achieved 87% sensitivity and 0.944 AUC using DCNN. Takumi et al. used a multilayer ANN on biopsy data, outperforming logistic regression.

3.5 Kidney Cancer

Research on kidney cancer detection primarily uses CT and MRI images, focusing on differentiate benign from malignant renal masses. Myronenko et al. used a CNN on the MICCAI 2019 dataset, achieving Dice scores of 0.9742 (kidney) and 0.8103 (tumor). Kang et al. combined ConvLSTM with 3D CNN, achieving 96.39% accuracy. Yanga et al.'s multi-scale residual CNN improved segmentation with a Dice score of 0.9390. Dihong et al. used a deep supervision-enhanced 3D U-Net, scoring 0.969 and 0.805. Zhou et al. used Inception V3 on CT slices, achieving 97% accuracy and 93% MCC with ROI data.

Zhao et al. applied 3D U-Net and ResNet to CT images, achieving Dice of 0.99 and up to 91.9% accuracy. Zabihollahy et al. used voting-based 3D CNNs on contrast-enhanced CT (5), achieving 83.75% accuracy. Türk et al.'s hybrid V-Net scored 0.97 (kidney) and 0.86 (tumor). Uhlig et al. used radiomics with ML, where random forest performed best (AUC 0.68, sensitivity 88%). Hea et al. used Raman spectroscopy and SVM, reaching 92.89% accuracy. Gong et al. proposed a 2D SCNet with 99.5% accuracy, and Pedersen et al. used ResNet50V2 to differentiate oncocytoma and RCC, with AUCs up to 0.991. Vendrami et al. applied MRI with random forest, achieving 81.2% accuracy.

3.6 Liver Cancer

Manual liver tumor tracing is time-consuming and reliant on radiologist expertise, highlighting the need for automatic segmentation using CT, MRI, and ultrasound. Hamm et al. used CNNs to classify hepatic lesions on MR images with 92% accuracy and sensitivity. Wang et al. achieved 76.5% PPV and 82.9% sensitivity in identifying lesion features. Shi et al. used CT images with dense networks and multi-phase input, reaching up to 85.6% accuracy and 0.925 AUC. Das et al. combined thresholdings with fuzzy clustering, yielding 95.02% accuracy with a C4.5 DT.

Araújo et al. applied RetinaNet and U-Net architectures, achieving a Dice score of 82.99%. Alirr et al. implemented dual U-Nets for liver and tumor segmentation with Dice scores of 95.6% and 70% (LiTS dataset). Zhen et al.'s deep learning system classified liver CT images with AUCs up to 0.998. Naeem et al. fused MRI and CT data, with MLP achieving up to 97.44% accuracy. Schmauch et al. used ResNet50 on ultrasound images, scoring 93.5% and 91.6% across various tasks. Mitrea et al. and Brehar et al. applied CNNs and comparative DL/ML methods on ultrasound images, achieving $\geqslant$97% and $\geqslant$90% accuracy, respectively. Yamakawa et al. developed a CAD system with VGGNet, reaching up to 98.1% accuracy.

3.7 Lung Cancer

Early lung cancer detection is crucial for survival, and CT/PET-CT imaging plays a key role. Lakshmanaprabu et al. used a DNN with linear discrimination and gravitational search, achieving 94.56% accuracy. Delzell et al. tested multiple ML classifiers, with SVM and elastic net reaching an AUC of 0.72. Khan et al. used SVM with 98.98% accuracy, while Saba et al. achieved 100% accuracy using multiple classifiers. Naqi et al. applied a hybrid model with AdaBoost, yielding 99% accuracy.

Asuntha et al. used FPSO to simplify CNNs and achieved 94.97% accuracy. Roy et al.'s fuzzy inference system reached 94.12% accuracy, and Orozco et al. used wavelet features with SVM for 80% precision and 90.9% sensitivity. Bhuvaneswari applied a genetic KNN with 90% accuracy, and Sangamithraa used fuzzy K-means and backpropagation with 90.7% accuracy. Makaju used watershed segmentation and SVM, achieving 86.6%.

Bębas et al. targeted non-small cell carcinoma using ML, reaching 75.48% accuracy. Chen proposed a hybrid 2D/3D CNN model with a dice score of 0.888 and 87.2% sensitivity. Zhang's four-channel CNN reduced false positives to 98.7% efficiency. Han et al. applied ML and VGG16 on PET/CT, achieving 84.1% accuracy and AUC 0.903. Schwyzer compared OSEM and BSREM (AUC 0.796 and 0.848). Finally, Wang et al.'s ConvPath software, using CNNs on pathology slides, reached 92.9% training and 90.1% testing accuracy.

IV Conclusions

This methodical review examine the use of AI in early detection across twelve common cancers, highlighting AI's potential to improve diagnostic accuracy and support radiologists by rapidly analyzing large datasets. The study found CT and ultrasound to be the most frequently used imaging modalities, while MRI, PET, and PET-CT were applied for detailed grading and treatment assessment (6). Mammography (X-rays) was used only in breast cancer studies, and AI was also applied to pathology, colposcopy, and biopsy images.

AI was most extensively applied in breast, brain, lung, and thyroid cancers, with significant use of both ML and DL techniques. Moderate research was observed in prostate, liver, kidney, and pancreatic cancers, while endometrial, cervical, and colorectal cancers relied more on pathology-based imaging. Bladder cancer had the least AI-based research, with limited use of DL algorithms.

REFERENCES

[1] Vogelstein B, Kinzler KW (1993) The multistep nature of cancer. Trends Genet 9:138–141.
[2] Ghafoor S, Burger IA, Vargas AH (2019) Multimodality imaging of prostate cancer. J Nucl Med 60:1350–1358.
[3] Batouty NM, Saleh GA, Sharafeldeen A, et · al (2022) State of the Art: Lung Cancer Staging Using Updated Imaging Modalities. Bioengineering (Basel) 9:493.